

Pairing effect on the giant dipole resonance width at low temperature

Nguyen Dinh Dang

RI-beam factory project office, RIKEN, 2-1 Hirosawa, Wako, 351-0198 Saitama, Japan

Akito Arima

House of Councilors, 2-1-1 Nagata-cho, Chiyoda-ku, Tokyo 100-8962, Japan

(Received 26 February 2003; revised manuscript received 2 July 2003; published 9 October 2003)

The width of the giant dipole resonance (GDR) at finite temperature T in ^{120}Sn is calculated within the phonon damping model including the neutron thermal pairing gap determined from the modified BCS theory. It is shown that the effect of thermal pairing causes a smaller GDR width at $T \lesssim 2$ MeV as compared to the one obtained by neglecting pairing. This improves significantly the agreement between theory and experiment, including the most recent data point at $T=1$ MeV.

DOI: 10.1103/PhysRevC.68.044303

PACS number(s): 24.30.Cz, 24.10.Pa, 21.60.-n, 24.60.Ky

I. INTRODUCTION

Intensive experimental studies of highly excited nuclei during the last two decades have produced many data on the evolution of the giant dipole resonance (GDR) as a function of temperature T and spin. The data show that the GDR width increases sharply with increasing T from $T \gtrsim 1$ MeV up to ≈ 3 MeV. At higher T a width saturation has been reported (See Ref. [1] for the most recent review). The increase of the GDR width with T is described reasonably well within the thermal shape-fluctuation model [2] and the phonon damping model (PDM) [3–5]. The thermal shape-fluctuation model assumes an adiabatic coupling of GDR to quadrupole degrees of freedom with deformation parameters β and γ induced by thermal fluctuations and high spins in the intrinsic frame of reference. Although this model shows an increase of the GDR width with T comparable with the experimental systematic at $1.2 \lesssim T \lesssim 3$ MeV, the GDR shapes generated using the strength function of this model differ significantly from the experimental ones [6]. The PDM considers the coupling of the GDR to pp and hh configurations at $T \neq 0$ as the mechanism of the width increase and saturation. The PDM calculates the GDR width and strength function directly in the laboratory frame without any need for an explicit inclusion of thermal fluctuation of shapes. The PDM reproduces fairly well both of the observed width [3,4] and shape [5,7] of the GDR at $T \neq 0$.

In general, pairing was neglected in the calculations for hot GDR as it was believed that the gap vanishes at $T = T_c < 1$ MeV according to the temperature BCS theory. However, it has been shown in Ref. [8] that thermal fluctuations smear out the superfluid-normal phase transition in finite systems so that the pairing gap survives up to $T \gtrsim 1$ MeV. This has been confirmed microscopically in the recent modified Hartree-Fock-Bogoliubov (HFB) theory at finite T [9], whose limit is the modified-BCS theory [10,11]. Other approaches such as the static-path approximation [12], shell-model calculations [13], as well as the exact solution of the pairing problem [14] also show that pairing correlations do not abruptly disappear at $T \neq 0$. It was suggested in Ref. [15] that the decrease of the pairing gap with increasing T ,

which is also caused by pp and hh configurations at low T , may slow down the increase of the GDR width. By including a simplified T -dependent pairing gap in the CASCADE calculations using the PDM strength functions, Ref. [7] has improved the agreement between the calculated GDR shapes and experimental ones.

Very recently the γ decays were measured in coincidence with ^{17}O particles scattered inelastically from ^{120}Sn [16]. A GDR width of around 4 MeV has been extracted at $T = 1$ MeV, which is smaller than the value of ~ 4.9 MeV for the GDR width at $T=0$. This result and the existing systematic for the GDR width in ^{120}Sn up to $T \approx 2$ MeV are significantly lower than the prediction by the thermal shape-fluctuation model. Based on this, Heckman *et al.* [16] concluded that the narrow width observed in ^{120}Sn at low T is not understood. The aim of the present work is to show that it is thermal pairing that causes the narrow GDR width in ^{120}Sn at low T . For this purpose we include the thermal pairing gap obtained from the modified-BCS theory [9–11] in the PDM [3–5], and carry out the calculations for the GDR width in ^{120}Sn at $T \leq 5$ MeV.

The paper is organized as follows. Section I summarizes the main equations for the GDR including thermal pairing within the PDM and discusses in detail the physical assumptions of the PDM. Section II analyzes the results of calculations of GDR width, energy, and cross section for ^{120}Sn at finite temperature in comparison with the most recent experimental systematic. The paper is summarized in the last section, where conclusions are drawn.

II. MAIN EQUATIONS FOR HOT GDR WITHIN PHONON DAMPING MODEL**A. Equations for GDR width and energy including thermal pairing**

The quasiparticle representation of the PDM including pairing has been already reported in Ref. [17]. Therefore we discuss here only the final equations, which will be used in numerical calculations. According to this formalism the GDR width Γ_{GDR} is presented as the sum of quantal (Γ_{Q}) and thermal (Γ_{T}) widths as [3–5,17]

$$\Gamma_{\text{GDR}} = \Gamma_{\text{Q}} + \Gamma_{\text{T}}, \quad (1a)$$

$$\Gamma_{\text{Q}} = 2\pi F_1^2 \sum_{ph} [u_{ph}^{(+)}]^2 (1 - n_p - n_h) \delta(E_{\text{GDR}} - E_p - E_h), \quad (1b)$$

$$\Gamma_{\text{T}} = 2\pi F_2^2 \sum_{s>s'} [v_{ss'}^{(-)}]^2 (n_{s'} - n_s) \delta(E_{\text{GDR}} - E_s + E_{s'}), \quad (1c)$$

where $(ss') = (pp')$ and (hh') with p and h denoting the orbital angular momenta j_p and j_h for particles and holes, respectively. The quantal and thermal widths come from the couplings of quasiparticle pairs $[\alpha_p^\dagger \otimes \alpha_h^\dagger]_{LM}$ and $[\alpha_s^\dagger \otimes \tilde{\alpha}_{s'}]_{LM}$ to the GDR, respectively. At zero pairing they correspond to the couplings of ph pairs, $[a_p^\dagger \otimes \tilde{a}_h]_{LM}$, and pp (hh) pairs, $[a_s^\dagger \otimes \tilde{a}_{s'}]_{LM}$, to the GDR, respectively (The tilde \sim denotes the time-reversal operation). The quasiparticle energies $E_j = [(\epsilon_j - \bar{\mu})^2 + \bar{\Delta}^2]^{1/2}$ are found from the modified-BCS equations (39) and (40) of Ref. [11], which determine the modified thermal gap $\bar{\Delta}$ and chemical potential $\bar{\mu}$ from the single-particle energies ϵ_j and particle number N . From them one defines the Bogoliubov coefficients u_j , v_j , and the combinations $u_{ph}^{(+)} = u_p v_h + v_p u_h$, and $v_{ss'}^{(-)} = u_s u_{s'} - v_s v_{s'}$. The quasiparticle occupation number n_j is calculated as [4]

$$n_j = \frac{1}{\pi} \int_{-\infty}^{\infty} \frac{n_{\text{F}}(E) \gamma_j(E)}{[E - E_j - M_j(E)]^2 + \gamma_j^2(E)} dE, \quad (2)$$

$$n_{\text{F}}(E) = (e^{E/T} + 1)^{-1},$$

where $M_j(E)$ is the mass operator and $\gamma_j(E)$ is the quasiparticle damping, which is determined as the imaginary part of the analytic continuation of $M_j(E)$ into the complex energy plane. These quantities appear due to coupling between quasiparticles and the GDR. Their explicit expressions are given by Eqs. (3) and (4) of Ref. [3], respectively, in which E_s is now the quasiparticle energy E_j . From Eq. (2) it is seen that the functional form for the occupation number n_j is not given by the Fermi-Dirac distribution $n_{\text{F}}(E_j)$ for noninteracting quasiparticles. It can be approximately so if the quasiparticle damping $\gamma_j(E)$ is sufficiently small so that the Breit-Wigner-like kernel under the integration can be replaced with the δ function. Equation (2) also implies a zero value for n_j in the ground state, i.e. $n_j(T=0)=0$. In general, it is not the case because of ground-state correlations (see, e.g., Refs. [10,18,19]). They lead to $n_j(T=0) \neq 0$, which should be found by solving self-consistently a set of nonlinear equations within the renormalized random-phase approximation (renormalized RPA). Within the RPA the equation for n_j yields the approximate expression

$$n_j(T=0) \simeq \sum_{j_j'} (2J+1)/(2j+1) [Y_{j_j'}^{(J)}]^2,$$

where $Y_{j_j'}^{(J)}$ is the RPA backward-going amplitude (J is the multipolarity). Since for collective high-lying excitations such as GDR one has $|Y_{j_j'}^{(J)}| \ll 1$, we expect the value $n_j(T=0)$ to be negligible.

The GDR energy E_{GDR} is found as the solution of the equation

$$\omega - \omega_q - P(\omega) = 0, \quad (3)$$

where ω_q is the unperturbed phonon energy and $P(\omega)$ is the polarization operator:

$$P(E) = F_1^2 \sum_{ph} \frac{[u_{ph}^{(+)}]^2 (1 - n_p - n_h)}{E - E_p - E_h} - F_2^2 \sum_{s>s'} \frac{[v_{ss'}^{(-)}]^2 (n_s - n_{s'})}{E - E_s + E_{s'}}. \quad (4)$$

Note that, in general, there are also backward-going processes leading to the terms $\sim \delta(\omega + E_p + E_h)$ and $\delta(\omega + E_s - E_{s'})$ as has been shown in Eqs. (14) and (15) of Ref. [17]. However, as the maximum of these terms is located at negative energy $\omega = -(E_p + E_h) < 0$ and $\omega = -(E_s - E_{s'}) < 0$, respectively, their contribution to the GDR, which is located at $\omega = E_{\text{GDR}} \gg 1$ MeV, is negligible. Therefore these backward-going processes are omitted here. It is now easy to see that, at zero pairing $\bar{\Delta}=0$, one has $u_p = 1$, $v_p = 0$, $u_h = 0$, $v_h = 1$ so that $[u_{ph}^{(+)}]^2 = 1$, $[v_{ss'}^{(-)}]^2 = 1$. As for the single-particle occupation number f_j , one obtains $f_h = 1 - n_h$ and $f_p = n_p$. The PDM equations for $\bar{\Delta}=0$ in Refs. [3,4] are then easily recovered from Eqs. (1)–(4).

B. Assumptions of phonon damping model

The PDM is based on the following assumptions.

(i) The matrix elements for the coupling of GDR to non-collective ph configurations, which causes the quantal width Γ_{Q} (1b), are all equal to F_1 . Those for the coupling of GDR to pp (hh), which causes the thermal width Γ_{T} (1c), are all equal to F_2 . The assumption of a constant coupling strength is well justified when the width of a collective mode is much smaller than the energy range ΔE (of order of E_{GDR}) over which this mode is coupled to the background states (the so-called weak coupling limit discussed in Refs. [13,20]).

(ii) It is well established that the microscopic mechanism of the quantal (spreading) width Γ_{Q} (1b) comes from quantal coupling of ph configurations to more complicated ones, such as $2p2h$ ones. The calculations performed in Refs. [21,22] within two independent microscopic models, where such couplings to $2p2h$ configurations were explicitly included, have shown that Γ_{Q} depends weakly on T . The microscopic study in Ref. [20], where a hierarchy of states of increasing complexity located around E_{GDR} is considered, has also confirmed the near constancy of Γ_{Q} . It also indicated that the width of a collective vibration does not depend on the detailed coupling to the compound nuclear eigenstates. Therefore, in order to avoid complicated numerical calculations, which are not essential for the increase of Γ_{GDR} at $T \neq 0$, such microscopic mechanism is not included within PDM, assuming that Γ_{Q} at $T=0$ is known. The model param-

eters are then chosen so that the calculated Γ_Q and E_{GDR} reproduce the corresponding experimental values at $T=0$ (see below).

Assumption (i) is satisfied for F_1 since the quantal width Γ_Q does not exceed 4.9 MeV. The PDM calculations in fact have shown that Γ_Q decreases from 4.9 MeV at $T=0$ to around 2.5 MeV at $T=5$ MeV for ^{120}Sn due to thermal effects in the factor $1-n_p-n_h$ (see the dashed line in Fig. 1(a) of Ref. [3] for zero pairing). A similar trend was also observed in the microscopic calculations of Ref. [21], where it was found that the GDR width at $T=3$ MeV is in fact smaller than at $T=0$ (see Figs. 9 and 10 of Ref. [21] and the discussion therein). That is why $\Gamma_Q(T=0)$ cannot be simply taken as a parameter uniformly added to what is calculated for Γ_T at $T \neq 0$ since a width $\Gamma_Q(T)=\Gamma_Q(T=0)$ would lead to a larger value for the total width Γ_{GDR} (1a) at higher T , worsening the agreement with the data.

Assumption (i) becomes poor for F_2 at $T \geq 3$ MeV, when the thermal width Γ_T is larger than 10 MeV (see the dotted line in Fig. 1(a) of Ref. [3]). Within such a large width one expects a considerable change of the level density of background states. To be quantitatively precise, one needs to use a self-consistent theory for the strength function, which includes the coupling to doorway states as in Ref. [20]. Such a theory is valid for any ratio of $\Gamma_{\text{GDR}}/\Delta E$. However, from assumption (ii) it also follows that the increase of Γ_{GDR} is now driven mainly by the thermal width Γ_T due to the factor $n_{s'}-n_s$. The change of n_j implies a change of the quasiparticle entropy S_{qp} . The latter is ultimately related to the change of the level density of background states within the realistic mean-field basis. This can be seen as follows. The complexity of the background states is measured by the information entropy S_{inf} of individual wave functions, which reflects the complicated relationship between the eigenbasis and representation basis. Meanwhile, the thermodynamic entropy S_{th} of the total system is directly determined by its statistical weight $\Omega(E)=\rho(E)\delta(E)$ as $S_{\text{th}}=\ln \Omega(E)$, where $\rho(E)$ is the level density. In a situation with incomplete information, such as in the statistical description of hot nuclei considered here, individual compound systems are replaced with a grand canonical ensemble of nuclei in thermal equilibrium. The probability for a quantum system to have a given eigenenergy is determined by the density matrix \mathcal{D} rather than by a pure wave function. The expectation value $\langle O \rangle$ of an observable O is given as the statistical average over the grand canonical ensemble $\langle O \rangle = \text{Tr}(\mathcal{D}O)$, which is derived from the maximum of the thermodynamic entropy $S_{\text{th}} = -\text{Tr}(\mathcal{D} \ln \mathcal{D})$. The modern shell-model calculations in Ref. [13] have shown that these three apparently different entropies, S_{qp} , S_{inf} , and S_{th} , behave very similarly for the majority of states in the realistic mean field consistent with residual interactions (see column II of Fig. 56 in Ref. [13] and the discussion therein). Significant differences between them take place only when the residual interaction beyond the mean field is very weak (see column I of Fig. 56 in Ref. [13]) or when the quasiparticle mean-field is absent (S_{inf} reaches its chaotic limit) (see column III of Fig. 56 in Ref. [13]). This might be the reason why the numerical results performed so far within the zero-pairing PDM [3–5] using assumptions (i)

and (ii) fit fairly well the experimental systematic for the GDR width including the existing data on the width saturation at $T \geq 3$ MeV. This is partly also due to the large experimental error bars for the extracted GDR width at high T (see, e.g., Refs. [23,24]). Therefore, at $T \geq 3$ MeV the results obtained under these assumptions should be considered as qualitative. This does not affect our present study of the pairing effect as the latter is significant only at low temperature ($T < 2.5$ MeV).

Within assumptions (i) and (ii) the model has only three T -independent parameters, which are the unperturbed phonon energy ω_q , F_1 , and F_2 . The parameters ω_q and F_1 are chosen so that after the ph -GDR coupling is switched on, the calculated GDR energy E_{GDR} and width Γ_{GDR} reproduce the corresponding experimental values for GDR in the ground state. At $T \neq 0$, the coupling to pp and hh configurations is activated. The F_2 parameter is then fixed at $T=0$ so that the GDR energy E_{GDR} does not change appreciably with varying T . The values of the PDM parameters for ^{120}Sn are given in Ref. [4] for the zero-pairing case.

In Ref. [4] we have presented an argument that, in our opinion, the effect due to coupling of GDR to noncollective ph , pp , and hh configurations at $T \neq 0$ within the PDM is tantamount to that of thermal shape fluctuations. This has been demonstrated by expanding the coupling of GDR phonon to noncollective ph , pp , and hh configurations into couplings to different multipole fields (see pages 437 and 438 of Ref. [4]). In this expansion the pp (hh)-pair operator $B_{ss'}^\dagger \equiv a_s^\dagger a_{s'}$ is expanded in terms of the tensor products of two ph -pair operators (see mappings (22) and (23) of Ref. [19]). Each ph -pair operator $B_{ph}^\dagger \equiv a_p^\dagger a_h$ can be then expressed in terms of the RPA phonon operators Q_q^\dagger and Q_q with RPA amplitudes X_{ph}^q and Y_{ph}^q . This leads to Eq. (2.43) in Ref. [4] for the part of the PDM Hamiltonian which describes coupling between the phonon and single-particle fields. Hence if Q_q^\dagger and Q_q are GDR phonon operators, $\{Q_{q_1}^\dagger, Q_{q_1}\}$ and $\{Q_{q_2}^\dagger, Q_{q_2}\}$ in Eq. (2.43) of Ref. [4] can have the moment and parity equal to $(1^-, 2^+)$, $(2^+, 3^-)$, etc. to preserve the total momentum $\lambda^\pi = 1^-$. Therefore, although $F_{ss'}^{(q)}$ are dipole matrix elements, the amplitudes $X_{ph}^{q_i}$ and $Y_{ph}^{q_i}$ ($i=1,2$) can be calculated microscopically, using the dipole-dipole, quadrupole-quadrupole, octupole-octupole, etc. components of residual interaction. This means that coupling to pp and hh configurations already includes in principle the coupling to different multipole-multipole fields via multiphonon configuration mixing at $T \neq 0$.¹

¹In Ref. [25] a version of PDM, which explicitly includes coupling to two-phonon configurations in the second order of the interaction vertex, was proposed. Expressions (2.17) and (2.18) of Ref. [25] derived for the polarization operator show that the width increase is still driven mainly by the factor $(n_s - n_{s'})$. The calculations with the GDR coupled to the first quadrupole phonon 2_1^+ required the energy $\omega_{2_1^+}$ and the ratio $r = F_i^{(2)}/F_i^{(1)}$ ($i=1,2$) to be fixed as additional parameters. A similar quality for the description of the experimental data for the temperature dependence of the GDR width has been restored after a reduction of the dipole matrix elements $F_1^{(1)} \equiv F_1$ and $F_2^{(1)} \equiv F_2$.

CASCADE calculations using PDM strength functions have produced the GDR shapes in good agreement with the experimental data for ^{120}Sn at $T > 1.54$ MeV (see Fig. 2 of Ref. [7]). The discrepancy at $T \leq 1.54$ MeV is due to omission or improper inclusion of pairing at low T , which is now studied in the present work. The splitting of GDR into two peaks is also clearly seen in the PDM calculations for ^{106}Sn [26]. These evidences are in favor of the argument discussed above and in Ref. [4].

Nonetheless, we recognize that the issue of whether coupling to pp and hh configurations at $T \neq 0$ is a microscopic (although indirect) interpretation of thermal shape fluctuations within the PDM is still not settled. The question of whether thermal shape fluctuations need to be included additionally within PDM or not remains to be investigated. The thermal shape-fluctuation model calculates the time-correlation function of the GDR by replacing the microcanonical ensemble with an ensemble of macroscopic variables, which are the deformation parameters (β, γ) in the body-fixed (principal axes) frame of reference (intrinsic frame). It parametrizes *a priori* the dipole correlation tensor by a frequency $E_k = E_0 \exp[-\sqrt{5/4\pi}\beta \cos(\gamma + 2/3\pi k)]$ and a width equal to $\Gamma_k = \Gamma_0 (E_k/E_0)^{1.8}$ along each i th semiaxis [2]. The effect of thermal fluctuations in this model is included via fluctuations of shapes by employing the macroscopic Landau theory of phase transitions [27]. Therefore, an explicit inclusion of thermal shape fluctuations in the PDM will bring in additional degrees of freedom, which increase the number of parameters of the model. At the same time, in a way similar to that mentioned in the footnote above, this will certainly require a renormalization of the existing parameters of the PDM to restore the agreement with the experimental systematic. While this issue is left open for future study, it does not affect the study of the role of thermal pairing in the present paper, since, as will be seen below, in order to describe the GDR width at low T , it is necessary to include thermal pairing in any model, whether it is the PDM or thermal shape-fluctuation one.

III. ANALYSIS OF NUMERICAL CALCULATIONS

A. Role of thermal pairing gap at low temperature

Shown in Fig. 1 is the T dependence of the neutron pairing gap $\bar{\Delta}_\nu$ for ^{120}Sn , which is obtained from the modified-BCS equations [9–11] using the single-particle energies determined within the Woods-Saxon potential at $T=0$. They span a space from ~ -40 MeV up to ~ 17 MeV, including seven major shells and $1j_{15/2}$, $1i_{11/2}$, and $1k_{17/2}$ levels. The pairing parameter G_ν is chosen to be equal to 0.13 MeV, which yields $\bar{\Delta}(T=0) \equiv \bar{\Delta}(0) \approx 1.4$ MeV. In difference with the BCS gap (dotted line), which collapses at $T_c \approx 0.79$ MeV, the gap $\bar{\Delta}$ (solid line) does not vanish, but decreases monotonously with increasing T at $T \geq 1$ MeV, resulting in a long tail up to $T \approx 5$ MeV. This behavior is caused by the thermal fluctuation of quasiparticle number, $\delta\mathcal{N}^2 \equiv \sum_j \delta\mathcal{N}_j^2$, where $\delta\mathcal{N}_j^2 = n_j(1-n_j)$ is the quasiparticle-number fluctuation on j th orbital. The latter is incorporated

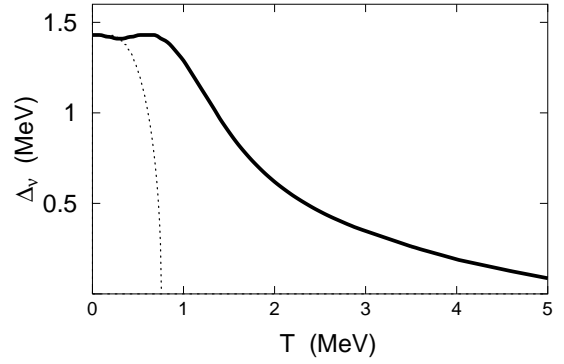


FIG. 1. Neutron pairing gap as a function of T . Solid and dotted lines show the modified-BCS gap $\bar{\Delta}$ and BCS gap, respectively.

as $\delta\mathcal{N}_j$ in the modified-BCS gap $\bar{\Delta}$ (see the last term at the right hand side of Eq. (39) of Ref. [11]).

To analyze the qualitative effect of thermal pairing on the GDR width we plot the usual single-particle occupation number $f_j = u_j^2 n_j + v_j^2 (1 - n_j)$ with n_j obtained within the modified-BCS theory [$\gamma_j(E) = 0$] as a function of single-particle energy ϵ_j for the neutron levels around the chemical potential in Fig. 2. It is seen that, in general, the pairing effect always goes counter to the temperature effect on f_j , causing a steeper dependence of f_j on ϵ_j . Decreasing with increasing T , this difference becomes small at $T \geq 3$ MeV. Since a smoother f_j enhances the pp and hh transitions leading to the thermal width Γ_T , pairing should reduce the GDR width, and this reduction is expected to be stronger at a lower T , provided the GDR energy E_{GDR} is the same. A deviation from this general rule is seen at very low $T \approx 0.1$ MeV, where the temperature effect is still so weak that f_j obtained at $\bar{\Delta} \neq 0$ (solid line) is smoother than that obtained at zero pairing (dotted line).

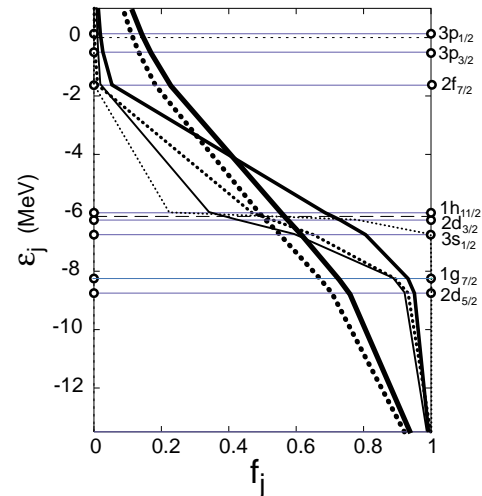


FIG. 2. (Color online) Single-particle occupation number f_j as a function of ϵ_j for the neutron levels around the chemical potential at $T=0.1, 1$, and 3 MeV. Results obtained including and without pairing are shown by solid and dotted lines, respectively (a thicker line corresponds to a higher T). The horizontal dashed line at ~ -6 MeV shows the chemical potential at $\bar{\Delta}=0$ and $T=0$.

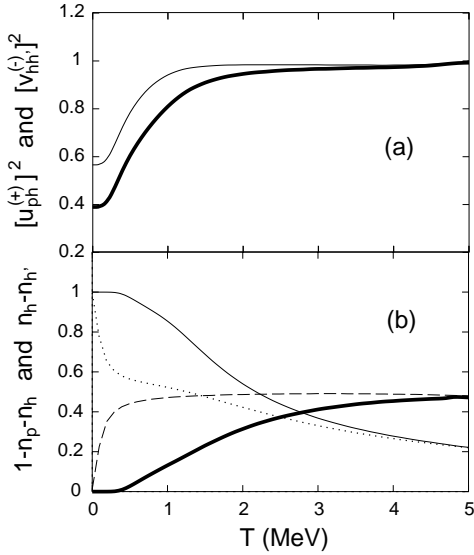


FIG. 3. Combinations of Bogoliubov coefficients (a) and quasiparticle occupations numbers (b). In (a), the thin and thick lines show $[u_{ph}^{(+)}]^2$ and $[v_{hh'}^{(-)}]^2$, respectively, for the orbits $p=2j_{7/2}$, $h=2d_{3/2}$, and $h'=1d_{5/2}$. In (b), the corresponding factors $1-n_p-n_h$ (thin line) and $n_h-n_{h'}$ (thick line) are shown. The factors f_h-f_p and $f_{h'}-f_h$ for the zero-pairing case are shown as the dotted and dashed lines, respectively.

To get an insight into the detail of the change of GDR width at low T we show in Fig. 3 the combinations $[u_{ph}^{(+)}]^2$ and $[v_{hh'}^{(-)}]^2$ of the Bogoliubov coefficients u_p , v_h , and $v_{h'}$ together with the factors $(1-n_p-n_h)$ and $(n_h-n_{h'})$ as well as their zero-pairing counterparts f_h-f_p and $f_{h'}-f_h$ for the particle $p=2j_{7/2}$, hole $h=2d_{3/2}$, and $h'=1d_{5/2}$ orbits as functions of T . The hole orbit $h=2d_{3/2}$ is located just below the chemical potential. Therefore the pairing effect is strongest for the ph and hh configurations involving this orbit. This figure shows a sharp increase of $[u_{ph}^{(+)}]^2$ and $[v_{ss'}^{(-)}]^2$ at $T \lesssim 1-2$ MeV due to a steep slope of the pairing gap, showing a strong pairing effect. At very low T , the numerator of the polarization operator (4) is close to $[u_{ph}^{(+)}]^2(E_p+E_h)$ because $1-n_p-n_h \approx 1$, while the thermal part $\sim (n_s-n_{s'}) \approx 0$. This value is equal to 3.67 MeV at $T=0.1$ MeV, which is smaller than $(\epsilon_h-\epsilon_p)=4.63$ MeV obtained at $\bar{\Delta}=0$. The denominator of Eq. (4) is also smaller than that obtained at $\bar{\Delta}=0$ because $E_p+E_h > \epsilon_h-\epsilon_p$ due to the gap. Therefore, at very low T , pairing may lead even to a smaller GDR energy. On the other hand, as $[u_{ph}^{(+)}]^2(1-n_p-n_h)$ and $[v_{ss'}^{(-)}]^2(n_s-n_{s'})$ are also smaller than f_h-f_p and $f_{s'}-f_s$, respectively, the competition of these effects in Eq. (1) can result in a larger width in the very low- T region. As T increases, the factor $1-n_p-n_h$ decreases while $[u_{ph}^{(+)}]^2$ increases to reach 1 at $T \gtrsim 2$ MeV because of the decreasing gap. This leads to the decrease of the quantal width Γ_Q . At the same time, coupling to pp and hh configurations starts to contribute due to the factor $(n_s-n_{s'})$. The combination $[v_{ss'}^{(-)}]^2$ also increases with T and reaches 1 at $T \gtrsim 3$ MeV. As the result, thermal width Γ_T starts to give an increasing contribution with T . However, as compared to

their zero-pairing counterparts, f_h-f_p and $f_{s'}-f_s$, the decrease of the quantal part $\sim (1-n_p-n_h)$ and increase of the thermal part $\sim (n_s-n_{s'})$ are much more moderate with increasing T up to 1 MeV. On the contrary, at $1 \leq T \leq 3$ MeV the decrease of $(1-n_p-n_h)$ and increase of $(n_s-n_{s'})$ with increasing T are steeper than their counterparts at $\bar{\Delta}=0$. At $T > 3-4$ MeV the total width approaches the saturation because of the dominating contribution of Γ_T , which ceases to increase due to the T dependence of $n_s-n_{s'}$ shown in Fig. 3(b) [3,4].

B. Temperature dependence of GDR width and energy

The GDR width Γ_{GDR} and energy E_{GDR} for ^{120}Sn were calculated from Eqs. (1) and (3), respectively, using the same set of PDM parameters ω_q , F_1 , and F_2 , which have been chosen for the zero-pairing case [3,4] (set A). The effect of quasiparticle damping is included in the calculations by using Eq. (2). The results are shown as the thin solid lines in Fig. 4. As seen from Fig. 4(b), the oscillation of GDR energy E_{GDR} with varying T occurs within the range of $\sim \pm 1.5$ MeV, which is wider compared with that obtained neglecting pairing. The latter is almost independent of T [dashed line in Fig. 4(b)]. As expected from the discussion above, the GDR energy E_{GDR} at $T=0.1$ MeV drops to 14 MeV, i.e., by 1.4 MeV lower than the GDR energy measured on the ground state. The GDR width increases to 5.3 MeV compared to 4.9 MeV on the ground state as shown in Fig. 4(a). At $0 \leq T \leq 0.5$ MeV, the above-mentioned competition between the decreasing quantal and increasing thermal widths makes the total width decrease first to reach a minimum of 3.4 MeV at $T \approx 0.2$ MeV then increase again with T . At $T \gtrsim T_c$ the width only increases with T . At $1 \leq T \leq 3$ MeV the GDR width obtained including pairing is smaller than the one obtained neglecting pairing [dashed line in Fig. 4(a)], but this difference decreases with increasing T so that at $T > 3$ MeV, when the gap $\bar{\Delta}$ becomes small, both values nearly coincide. This improves significantly the agreement with the experimental systematic at $1 \leq T \leq 2.5$ MeV. In order to have the same value of 4.9 MeV for the GDR width at $T=0$, we also carried out the calculation using slightly readjusted values $F_1' = 0.96F_1$ and $F_2' = 1.03F_2$ while keeping the same ω_q (set B). The result obtained is shown in the same Fig. 4 as the thick solid lines. The GDR energy E_{GDR} moves up to 16.6 MeV at $T=0.1$ MeV and at $T_c \leq T \leq 1.2$ MeV in agreement with the value of 16.5 ± 0.7 MeV extracted at $T=1$ MeV in Ref. [16]. The width at $T=1$ MeV also becomes slightly smaller, which agrees quite well with the latest experimental point [16]. At $T > 1$ MeV the results obtained using two parameter sets A and B are nearly the same. The effect of quantal fluctuations δN^2 of particle number within the BCS theory at $T=0$, however, is neglected in these results. To be precise, this effect should be included using the particle-number projection method at finite T . However, the latter is so computationally intensive that the calculations were carried out so far only within schematic models (see, e.g., Ref. [31]), or one major shell for nuclei with $A \leq 60$ as in the shell-model Monte Carlo method [32]. Therefore, for the limited purpose of the present study, assuming that $\delta N^2 \gg 1$, we applied the approximated projection at $T=0$ pro-

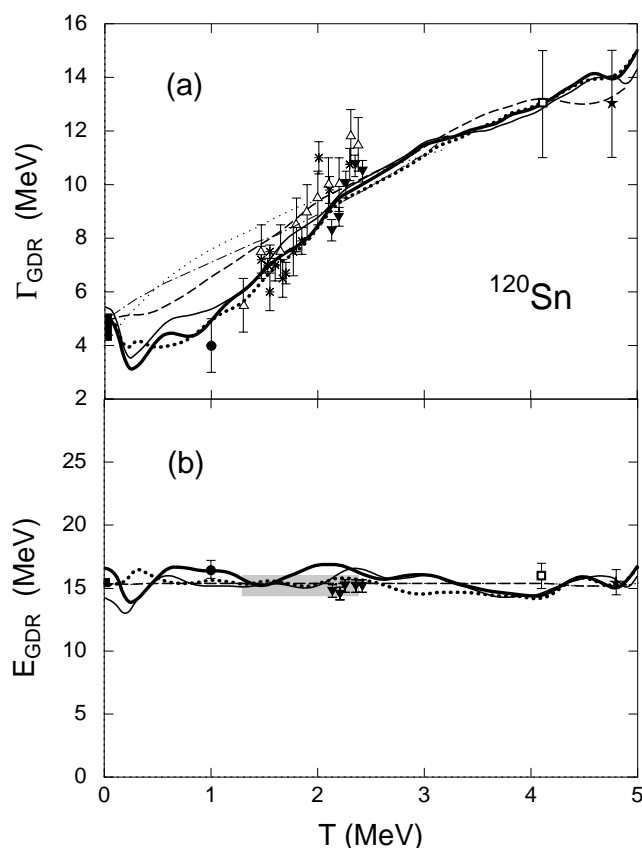


FIG. 4. GDR width Γ_{GDR} (a) and energy E_{GDR} (b) as functions of T for ^{120}Sn . The dashed lines show the PDM results obtained neglecting pairing (In (a) it is the same as the solid line with diamonds from Fig. 1(a) of Ref. [3]). The thin and thick solid lines are the PDM results including the gap $\bar{\Delta}$, which are obtained using the parameter sets A and B , respectively. The thick dotted lines are the PDM results including the renormalized gap $\tilde{\Delta}$ (see text). Solid circles are the low- T data from Ref. [16]. Crosses and open triangles in (a) are from Fig. 4 of Ref. [28]. The corresponding GDR energies decrease from 16 MeV to 14.5 MeV with increasing T as shown in the shaded rectangle in (b). Solid upside-down triangles are data from Ref. [29]. Open squares and stars are high- T data for ^{110}Sn from Refs. [23] and [24], respectively. Data at $T=0$ are for GDR built on the ground state of tin isotopes with masses $A=116$ – 124 from Ref. [30]. The predictions by two versions of the thermal shape-fluctuation model are shown in (a) as the dash-dotted [2] and thin dotted [28] lines, respectively.

posed in Ref. [33], which leads to the renormalization of the gap as $\tilde{\Delta}(T)=[1+1/\delta N^2]\bar{\Delta}$ with $\delta N^2=\bar{\Delta}(0)^2\sum_j(j+1/2)/[(\epsilon_j-\bar{\mu})^2+\bar{\Delta}(0)^2]$ [34]. This yields $\tilde{\Delta}(T=0)\approx 1.5$ MeV ($\delta N\approx\pm 4$). The PDM results obtained using the gap $\tilde{\Delta}$ and the parameter set B are shown in the same Fig. 4 as the thick dotted lines. The GDR width becomes 5 MeV with $E_{\text{GDR}}=15.3$ MeV at $T=0$ in good agreement with the GDR parameters extracted on the ground state. It is seen that the fluctuation of the width at $T\leq 0.5$ MeV is largely suppressed by using this renormalized gap $\tilde{\Delta}$. For comparison, the predic-

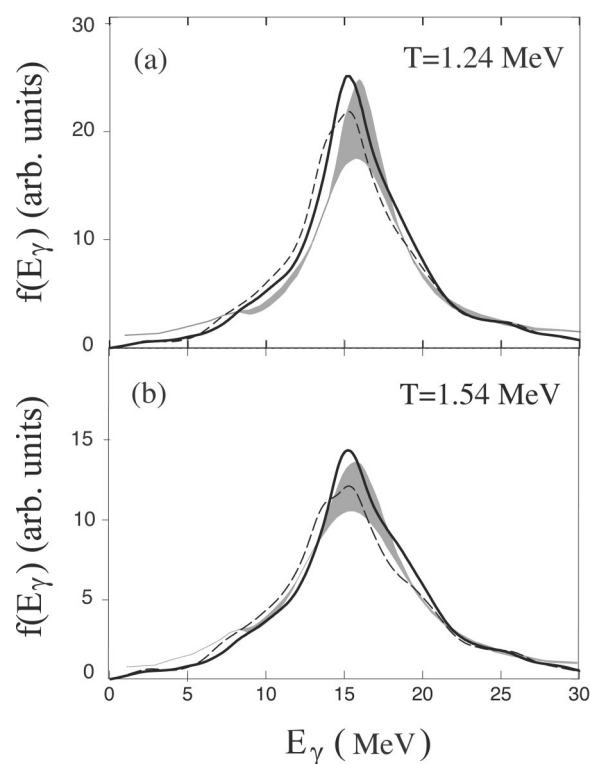


FIG. 5. Experimental (shaded areas) and theoretical divided spectra obtained without pairing (dashed lines) and including the gap $\bar{\Delta}$ (thick solid lines) as for the thick solid line in Fig. 4.

tions by two versions of thermal shape-fluctuation model [2,28] are also plotted in Fig. 4(a) as the dash-dotted [2] and thin dotted [28] lines. It is seen that these predictions, in particular the one given by the phenomenological version in Ref. [28], significantly overestimate the GDR width at low temperature $T\lesssim 1.3$ MeV. The predicted overall increase of the width is not as steep as the experimental systematic and the PDM prediction. The curvature of the trend is also opposite to the experimental one and that given by the PDM. It is, therefore, highly desirable to see how the prediction by the thermal shape-fluctuation model would change by taking into account the effect of thermal pairing gap discussed in the present work in combination with the use of a specific Hamiltonian to calculate every quantity [35].

C. Effect of thermal pairing on GDR cross section at low temperature

Shown in Fig. 5 are GDR cross sections obtained for ^{120}Sn using Eq. (1) of Ref. [7]. The experimental cross section are taken from Fig. 2 of Ref. [7]. They have been generated by CASCADE at excitation energies $E^*=30$ and 50 MeV, which correspond to $T_{\text{max}}=1.24$, and 1.54 MeV, respectively. The theoretical cross sections have been obtained using the PDM strength function $S_{\text{GDR}}(E_\gamma)$ from Eq. (2.22) of Ref. [5] at $T=T_{\text{max}}$. This is the low temperatures region, at which discrepancies are most pronounced between theory and experiment. (A divided spectrum free from detector re-

sponse at $T=1$ MeV is not available in Ref. [16].) From this figure it is seen that thermal pairing clearly offers a better fit to the experimental line shape of the GDR at low temperature. As has been discussed in Ref. [7], for an absolute comparison, the PDM strength functions for all decay steps starting from T_{\max} down to $T=0$ MeV should be included in the CASCADE to generate a divided spectra, which can be directly compared with the experimental ones. It is our wish that such calculations be carried out in collaboration with the authors of Ref. [16] in the near future.

IV. CONCLUSIONS

In this paper we have included the pairing gap, determined within the modified-BCS theory [10,11], in the PDM to calculate the width of GDR in ^{120}Sn at $T \leq 5$ MeV. In

difference with the gap given within the conventional BCS theory, which collapses at $T_c \approx 0.79$ MeV, the modified-BCS gap never vanishes, but monotonously decreases with increasing T up to $T=5$ MeV. The results obtained show that thermal pairing indeed plays an important role in lowering the width at $T \leq 2$ MeV as compared to the value obtained without pairing. This improves significantly the overall agreement between theory and experiment, including the width at $T=1$ MeV extracted in the latest experiment [16].

ACKNOWLEDGMENT

The numerical calculations were carried out using the FORTRAN IMSL Library 3.0 by Visual Numerics on the Alpha server 800 5/500 at the Division of Computer and Information of RIKEN.

-
- [1] M. N. Harakeh and A. van der Woude, *Giant Resonances—Fundamental High-frequency Modes of Nuclear Excitation* (Clarendon, Oxford, 2001).
- [2] W. E. Ormand, P. F. Bortignon, and R. A. Broglia, *Phys. Rev. Lett.* **77**, 607 (1966); W. E. Ormand *et al.*, *Nucl. Phys.* **A614**, 217 (1997).
- [3] N. D. Dang and A. Arima, *Phys. Rev. Lett.* **80**, 4145 (1998).
- [4] N. D. Dang and A. Arima, *Nucl. Phys.* **A636**, 427 (1998).
- [5] N. Dinh Dang, K. Tanabe, and A. Arima, *Nucl. Phys.* **A645**, 536 (1998).
- [6] G. Gervais, M. Thoennessen, and W. E. Ormand, *Phys. Rev. C* **58**, R1377 (1998).
- [7] N. Dinh Dang, K. Eisenman, J. Seitz, and M. Thoennessen, *Phys. Rev. C* **61**, 027302 (2000).
- [8] L. G. Moretto, *Phys. Lett.* **40B**, 1 (1972).
- [9] N. Dinh Dang and A. Arima, *Phys. Rev. C* **68**, 014318 (2003).
- [10] N. Dinh Dang and V. Zelevinsky, *Phys. Rev. C* **64**, 064319 (2001).
- [11] N. Dinh Dang and A. Arima, *Phys. Rev. C* **67**, 014304 (2003).
- [12] N. D. Dang, P. Ring, and R. Rossignoli, *Phys. Rev. C* **47**, 606 (1993).
- [13] V. Zelevinsky, B. A. Brown, N. Frazier, and M. Horoi, *Phys. Rep.* **276**, 85 (1996).
- [14] A. Volya, B. A. Brown, and V. Zelevinsky, *Phys. Lett. B* **509**, 37 (2001).
- [15] N. Dinh Dang, K. Tanabe, and A. Arima, *Nucl. Phys.* **A675**, 531 (2000).
- [16] P. Heckman *et al.*, *Phys. Lett. B* **555**, 43 (2003).
- [17] N. D. Dang, V. K. Au, T. Suzuki, and A. Arima, *Phys. Rev. C* **63**, 044302 (2001).
- [18] K. Hara, *Prog. Theor. Phys.* **32**, 88 (1964); K. Ikeda, T. Udagawa, and H. Yamamura, *ibid.* **33**, 22 (1965); D. J. Rowe, *Phys. Rev.* **175**, 175 (1968); J. Dukelsky and P. Schuck, *Nucl. Phys.* **A512**, 466 (1990).
- [19] F. Catara, N. Dinh Dang, and M. Sambataro, *Nucl. Phys.* **A579**, 1 (1994).
- [20] B. Lauritzen, P. F. Bortignon, R. A. Broglia, and V. G. Zelevinsky, *Phys. Rev. Lett.* **74**, 5190 (1995).
- [21] P. F. Bortignon, R. A. Broglia, and G. F. Bertsch, *Nucl. Phys.* **A460**, 149 (1986).
- [22] N. Dinh Dang, *Nucl. Phys.* **A504**, 143 (1989).
- [23] A. Bracco *et al.*, *Phys. Rev. Lett.* **62**, 2080 (1989).
- [24] J. J. Gaardhøje *et al.*, *Phys. Rev. Lett.* **59**, 1409 (1987).
- [25] N. Dinh Dang, K. Tanabe, and A. Arima, *Phys. Rev. C* **58**, 3374 (1998).
- [26] N. Dinh Dang, A. Ansari, and A. Arima, preprint RIKEN-AF-NP-361, 2000; N. Dinh Dang, *Nucl. Phys.* **A687**, 253C (2001).
- [27] L. D. Landau and E. M. Lifshitz, *Statistical Physics*, Course of Theoretical Physics Vol. 5 (Nauka, Moscow, 1964).
- [28] D. Kusnezov, Y. Alhassid, and K. A. Snover, *Phys. Rev. Lett.* **81**, 542 (1998), and references therein.
- [29] M. P. Kelly *et al.*, *Phys. Rev. Lett.* **82**, 3404 (1999).
- [30] B. L. Berman, *At. Data Nucl. Data Tables* **15**, 319 (1975).
- [31] R. Rossignoli, N. Canosa, and P. Ring, *Phys. Rev. Lett.* **80**, 1853 (1998).
- [32] Y. Alhassid, S. Liu, and H. Nakada, *Phys. Rev. Lett.* **83**, 4265 (1999).
- [33] I. N. Mikhailov, *Sov. Phys. JETP* **18**, 761 (1964).
- [34] N. D. Dang, *Z. Phys. A* **335**, 253 (1990).
- [35] A. Ansari, N. Dinh Dang, and A. Arima, *Phys. Rev. C* **62**, 011302(R) (2000); **63**, 024310 (2000).